

A state machine-based approach for estimating the capacity loss of Lithium-Ion Batteries

Ruth David¹ and Dirk Söffker²

^{1,2} *Chair of Dynamics and Control, University of Duisburg-Essen, 47057 Duisburg, Germany*
ruth.daivd@uni-due.de
soeffker@uni-due.de

ABSTRACT

The use of Lithium-Ion Batteries (LIBs) have increased in recent years in many applications such as hybrid electrical vehicles (HEV), consumer electronic equipment, and electricity grid. The batteries undergo degradation during usage due to material aging and electrochemical processes, leading to efficiency reduction of battery-powered systems as well as catastrophic events. Several stress factors such as battery temperature, ambient temperature, and C-rate in the loading profiles influence the degradation. Therefore, predicting the health of the battery has gained attention. The service life can be extended or a system failure can be avoided by maintenance measures precisely matched to the function loss or by changing usage strategies. The State-of Health (SoH) condition of the battery can be determined by the application of lifetime models. Various health indicators such as remaining useful lifetime (RuL) and capacity fade are determined by the models based on the stress factors (utilization variables). For optimal use of the battery, it is helpful to develop an accurate lifetime model to represent the dynamic properties. However, models developed are less computationally efficient and unable to represent the non-linear degradation behavior well. The development of a precise model with correct parameterization is also costly. This is particularly true for models developed based on physical and chemical properties of the battery. In this contribution, an artificial neural network (ANN)-based state machine approach is introduced for capacity fade estimation. The degradation process is represented using three states modeling three different levels and the progression from the first state to the last. Capacity associated with each state is described using the non-linear autoregressive neural network with external input (NARX). The NARX is selected due to its ability to accurately model non linear behavior and time series data. Unlike known models, which are developed using analytical mathematical equations

related to the battery properties, a combined machine learning approach is used here instead to learn the capacity behavior from historical data. Battery data sets from NASA are used for experimental verification. Based on the results, the estimated capacity fade show close proximity to actual capacity fade, with a low mean square error for different data sets. In addition, the estimated state progression follows the actual state progression.

1. INTRODUCTION

In recent years, the use of lithium-ion batteries (LIBs) in various systems have increased, such as in hybrid electrical vehicles (HEV), unmanned aerial vehicles, and telecommunication systems. This is due to its light weight, long cycle life, and low charge rate loss (Hu, Zou, Zhang, & Li, 2017; Xiao, 2015). These batteries provide energy through electrochemical processes during charging and discharging cycles. However, increasing the number of cycles causes aging as well as stability deterioration of the batteries from side reactions. Some of the common aging reactions include solid-electrolyte interface (SEI) layer growth, corrosion of lithium, and lithium plating (Daigle & Kulkarni, 2013). The SEI growth occurs on the negative electrode during cycling and storage at high temperatures, which causes impedance increase leading to deterioration (Daigle & Kulkarni, 2013). The corrosion of lithium also occurs in the negative electrode leading to capacity loss due to lithium-ion loss (Daigle & Kulkarni, 2013). Lithium layer plating is formed on the negative electrode due to low temperatures, high charge rates, and low cell voltages causing the loss of lithium ions as well (Daigle & Kulkarni, 2013). The degradation of the batteries are prone to catastrophic events such as the breakdown of a battery operated system and thermal runaway. Therefore, monitoring the battery's health is important for maintaining safety, the system's performance, and avoiding unexpected maintenance. Several health indicators such as remaining useful lifetime (RuL), capacity fade, and End-of-Lifetime (EoL) are used for monitoring the health.

Ruth David et al. This is an open-access article distributed under the terms of the Creative Commons Attribution 3.0 United States License, which permits unrestricted use, distribution, and reproduction in any medium, provided the original author and source are credited.

As part of the battery's prognosis and health management, many approaches have been proposed to estimate the health indicators using lifetime models. Generally, there are two types of approaches to develop these models: model-based (Christensen & Newman, 2003; Downey, Lui, Hu, Laflamme, & Hu, 2019) and data-driven (Zhang, Wu, Wang, & Chen, 2021; Catelani, Ciani, Fantacci, Patrizi, & Picano, 2021) approaches. One of the main challenges faced in the development of lifetime models is different LIBs have different lifetime expectancies affected by stress factors, such as battery surface temperature, ambient temperature, Depth-of-Discharge (DOD), and C-rates (Keil & Jossen, 2017; Waldmann, Wilka, Kasper, Fleischhammer, & Wohlfahrt-Mehrens, 2014). In addition, the limited aspects of various approaches makes it challenging to select the appropriate approach. For an example, certain model-based approaches are developed based on specific operating conditions, as shown in (Zheng, Zhang, Zhu, Wang, & Jiang, 2016) and (Ashwin, Chung, & Wang, 2016). Also, certain model-based approaches such as (Liu et al., 2017) require complicated electrochemical information and experiments. Both model-based and data-driven approaches tend to have difficulties in modeling complex non-linear degradation behaviors (Xu & Chen, 2017). Hence, there is a lack of suitable lifetime models in current literature for the estimation of the health indicators. Only a few approaches in literature have considered the damage states associated with the multi-switching degradation behavior of the battery. A new machine learning (ML)-based approach is introduced here to model the switching capacity fade using a state machine approach, such that different degradation states are modeled within one framework.

In this research, a non-linear auto regressive neural network with external input (NARX)-based state machine model is introduced for the capacity fade estimation (output). Different states of degradation are modeled using three discrete states, such that capacity fade associated with each state are estimated using the NARX model. Transition from the first state to the last are defined to show the damage progression. These transitions are based on specific threshold conditions (parameters) associated with the normalized battery's surface temperature (input) and actual capacity. As parameters of the model affect the estimation performance, developing optimal parameters are important. The parameters are optimized using a Non-dominated sorting genetic algorithm-II (NSGA-II) here.

The paper is structured as follows: In Section 2, the background of the battery aging and the different lifetime models are described. In Section 3, the NARX-based state machine approach is presented. In addition, optimization of parameters is detailed. The application of the method is discussed in Section 4, which entails the description of the experimental

data, training, and test procedures. In Section 5, the results are presented followed by a conclusion in Section 6.

2. BACKGROUND OF BATTERY AGING, LIFETIME MODELS, AND CURRENT DEVELOPMENTS

The correlation between various stress factors and battery aging is investigated in several research contributions. In (Keil & Jossen, 2017), the capacity fade dependence on different operating temperatures is studied. For instance, low temperatures generate an accelerated and increased capacity degradation during cycling aging (when load is applied). On the other hand, capacity degradation decreases at low temperatures during calendar aging (when no load is applied). Based on (Wang et al., 2011), high ambient temperatures (above room temperature) or very low temperatures (lower than zero) accelerate the aging process. In this research, the normalized battery's temperature is used as the model's input.

As mentioned, the battery's health can be stipulated by estimating the health indicators based on the mentioned stress factors using lifetime models, which are developed using either model-based or data-driven approaches. The model-based approaches are often based on the physical and chemical properties of the battery, given in (Downey et al., 2019). It is also based on observer design and parameter estimations (Plett, 2004). A drawback of this approach is it may not be appropriate for complex systems, as representing the degradation behavior based on physical and chemical aspects may not be suitable (J. Wu, Kong, Cheng, Yang, & Zuo, 2022). In addition, implementing parameters based on the electrochemical models is time consuming due to need of elaborate experimental setups, as stated in (Y. Wu, Li, Wang, & Zhang, 2019). The generalization of the models is also limited according to (J. Wu et al., 2022). Nevertheless, empirical model-based approaches (do not consider the battery's electrochemistry aspects) tend to be computationally efficient, as in (Saha & Goebel, 2009). Data-driven approaches (such as ML models) are often based on historical measured data. These models have the benefit of being computationally and time efficient, making the models suitable for larger systems (Zhao, Zhang, & Wang, 2022). The ML-based models have gained popularity in recent years as the electrochemistry knowledge is not needed. Some of the ML models used are ANN (Catelani et al., 2021; Zhao et al., 2022) and SVM (Patil et al., 2015). However, poor quality information collected can affect performance of data-driven models negatively. Hence, appropriate techniques needs to be implemented when collecting data. Overall, there is a lack of appropriate lifetime models to represent the degradation behavior of LIBs in current research due the limitations mentioned.

Unlike the aforementioned approaches, a state machine models the switching behaviors of a system using different states. Behaviors are modeled using discrete states that transition be-

tween each other based on the model's input and transition conditions (Gill, 1962). The approach has shown promising results in various areas, such as modeling plant growth based on water stress (Kögler & Söffker, 2020), tribological experiment damage behaviors (Beganovic & Söffker, 2017) as well as the estimation of human driving behaviors (David, Rothe, & Söffker, 2021). However, it has not been widely used in the degradation behavior of LIBs. This approach has certain advantages like its flexibility as states are defined abstractly (Lopes, Silva, & Monteiro, 2012) and easy determination of states (Micheli, Brayton, & Sangiovanni-Vincentelli, 1985).

Therefore, a new ML-based model is presented here, by combining the state machine approach (to model different degradation levels) and NARX neural network (to estimate the capacity fade). The NARX is beneficial when traditional methods are not adequate for applications with complex and non-linear relationships between the input and output. The method is also able to handle time series data well. In addition, it has a better computational efficiency than conventional recurrent networks (Siegelmann, Horne, & Giles, 1997). Furthermore, the gradient descent learning is more effective than other recurrent networks (Horne & Giles, 1994).

3. NARX-BASED STATE MACHINE LIFETIME MODEL

In this section, the battery lifetime model developed using a state machine-based NARX approach is introduced for the estimation of capacity fade and degradation levels. The discharge capacity is considered in this research. In addition, optimization of model parameters is described to develop an optimal model. The input of the model is the normalized battery temperatures and the output is the estimated capacity.

3.1. State machine approach

As mentioned, behaviors of multi-state switching systems can be modeled using state machine models with discrete states. The states transition from one state to another or remain in the same state determined by the model's inputs and transition conditions (Gill, 1962), (Wilson & Mantooh, 2013). The transition conditions are defined by designers. The model consists of three states, whereby each state represents different degradation levels/behaviors describing the aging. As input, only the normalized temperature of the battery is taken into account, due to the fact that the temperature change contributes to the capacity loss. The normalization is done with the z-score normalization. The transition conditions are defined using the normalized temperature and the End-of-Lifetime (EoL) capacity. The estimated loss of capacity associated with each state is modeled using a neural network model (NARX).

Based on Figure 1, when the current estimated state is state 1, it can transition to state 2 (EoL reached) if the transition conditions are met to estimate the next state and capacity fade.

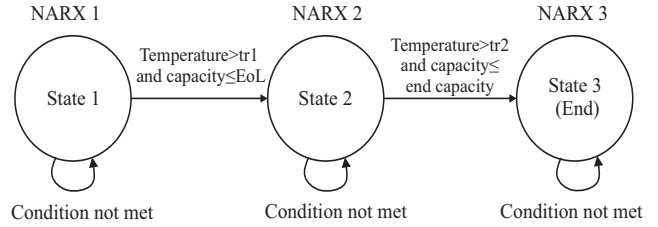


Figure 1. NARX-based state machine model.

Otherwise, the model remains in state 1. Similarly, possible estimations when the current estimated state is state 2 is transitioning to state 3 or remaining in state 2. If state 3 is estimated, the model can only remain in state 3 for the next estimation.

As for the transition conditions, if the normalized temperature is higher than threshold tr_1 and the capacity is less than or equals to the capacity at EoL (here: reaches 80 % of the nominal capacity), a state transition from state 1 to state 2 occurs (Figure 1). This indicates, the battery has reached EoL at state 2. On the other hand, a transition from state 2 to state 3 occurs when the temperature is higher than tr_2 and the capacity is less than or equals to the capacity measured at the final time point. Once state 3 has been reached, the model can only remain in the same state, as the final state has been reached. If conditions are not met, the model remains in the same state. The tr_1 and tr_2 (parameters of the model) are selected automatically using NSGA-II. These are given as unknown values to the algorithm initially. Based on different temperature ranges for the specific states and capacities, the algorithm selects and optimizes the threshold values.

3.2. Non-linear auto regressive neural network with external input (NARX)

The estimated capacity is calculated using different NARX models for each state, presented in Figure 1 (NARX 1, NARX 2, and NARX 3). Nevertheless, the structure of the model is the same for all states. Only the input and parameter values differ depending on the state. The NARX model describes the input-output mapping using a multi-layer perceptron (Chan, Yuen, Lee, & Arashpour, 2015). A usual NARX model also incorporates the time delays and feedback (target values or output, depending on the network type) in the input layer. The target values are the actual capacity values. In the model utilized an open loop network is used, which means only the input data variables (normalized battery's temperature) and target values (priori information of capacity) as feedback are used. The output is not fed back to the network (to the input layer), unlike a closed loop. The time delays of the input and target values are two time steps (1:2), which means the estimation starts at the third time step. The NARX network is trained to perform estimations of the capacity fade based on the past battery's temperature and target capacity

values. The NARX input-output relationship can be describe as (Venturini, 2005)

$$\hat{y}(t) = f[i(t), i(t-1), \dots, i(t-m_i), y(t-1), \dots, y(t-m_k)] + e(t), \quad (1)$$

whereby $\hat{y}(t)$ and $y(t)$ are the estimated and target values, $i(t)$ is the input, m_i and m_k are the time delays of the input and target variables respectively, t is the time step, and $e(t)$ is the error between the estimated and target values.

The network consists of inputs, targets, a hidden layer of ten neurons, and an output layer. In the NARX model, the input layer consists of two inputs: the normalized temperature and target capacity neurons. The activation function considered in this model is the tansig function (Hyperbolic tangent sigmoid transfer function). The value of each hidden layer neuron is calculated based on the inputs, targets, and weights associated between the neurons. In addition, the bias values are also taken into consideration. The capacity estimations are calculated based on the values of hidden layer neurons and weights associated between the hidden layer neurons and output neuron.

3.3. Parameter optimization and performance

The parameters of the network are the weights and biases related to the neural network as well as the temperature thresholds associated with the transition conditions in the state machine. These parameters affect the estimation performance, thus selecting optimal parameter values is important. Many optimization approaches have been employed to optimize the parameters, such as Particle Swarm Optimization in (Álvarez Antón et al., 2016). The algorithm may perform well in finding local optimum solutions, however the global optimum solution search capability is limited as it may get stuck in the local optima (Thangaraj, Pant, Abraham, & Snasel, 2012). In contrast, NSGA-II has a good performance in finding the global optimum (Deb, Pratap, Agarwal, & Meyarivan, 2002). Thus, the NSGA-II is used to select/optimize the parameter values here. This method is based on non-dominated sorting solutions and crowding distances. The main advantages of this method is its ability to solve multi-objective optimization problems, its elitism (which increases the convergence speed), and its ability to solve problems with non-feasible solutions (Deb et al., 2002). The objective function of the optimization is given as

$$obj(t) = (|actual\ capacity(t) - estimated\ capacity(t)|). \quad (2)$$

The objective function is chosen with respect to minimizing the deviation between the actual and estimated discharge ca-

pacities. To evaluate the overall performance of the model, the mean square error (MSE) and relative mean square error (RMSE) are often used, as done in (Catelani et al., 2021).

4. APPLICATION OF THE METHOD

The application of the proposed method is elaborated in this section. First, three experimental design of charging and discharging procedures are explained (Saha & Goebel, 2007; Bole, Kulkarni, & Daigle, 2014). Next, the training and test phases are explained.

4.1. Experimental setup

The battery data sets are obtained from NASA Prognostics Center of Excellence (PCoE) (Saha & Goebel, 2007; Bole et al., 2014). Six data sets based on three different experiments are defined as experiment I (Saha & Goebel, 2007), experiment II (Bole et al., 2014), and experiment III (Bole et al., 2014). Experiment I simulates a constant current (CC)-constant voltage (CV) charging and discharging process, which is non-dynamic. On the other hand, experiment II and III simulate a dynamic charging and discharging operation using a random walk (RW) process.

4.1.1. Experiment I

Experiment I utilizes two battery data sets (B0005 and B0006) (Saha & Goebel, 2007). The batteries are first charged using the CC mode at 1.5 A. When the battery voltage reaches 4.2 V, the charging switches to the CV mode until the current falls to 20 mA. Discharging process begins with the CC mode at 2 A until the voltage decreases to 2.7 V and 2.5 V for B0005 and B0018, respectively (Saha & Goebel, 2007). The nominal capacity of the batteries are 2 A. The EoL is reached when the capacity reaches 70% of the nominal capacity (1.44 A). The charging and discharging process do not simulate dynamical load profiles. The ambient temperature is room temperature.

4.1.2. Experiment II

Experiment II is based on a RW process. Two LIB data sets (RW 9 and RW 10) from the experiment are utilized in this contribution (Bole et al., 2014). The RW process is used to charge and discharge the batteries between -4.5 A and 4.5 A. After 1500 RW step cycles, a reference charge and discharge operation is done to evaluate the capacities. The EoL is defined when the capacity reaches 1.68 A for both batteries (80 % of the nominal capacity, as defined by battery manufacturers). The capacities are calculated based on the current and relative time.

Table 1. Training and test data sets for each experiment.

Training data sets	Test data sets
B0005	B0006
RW10	RW9
RW7	RW1

4.1.3. Experiment III

The batteries in Experiment III also undergo the RW operation. Two battery data sets (RW1 and RW7) are used (Bole et al., 2014). The RW is performed by charging the batteries for a randomly selected period between 0.5 and 3 hours. The batteries are then discharged using a randomly selected current between 0.5 A and 3 A. Following 50 RW cycles, a reference operation is done to evaluate the capacities. The EoL capacities are 1.60 A and 1.59 A (80 % of the nominal capacity) for RW1 and RW7, respectively. The capacities are calculated based on the current and relative time.

For experiments II and III, the batteries' temperature during the reference discharge operation is considered as input of the model. In addition, battery temperatures are in degree Celsius ($^{\circ}\text{C}$). Capacity fade is observed throughout the discharge phase for all experiments.

4.2. Training and test

For each experiment, the temperature values of one battery data set are used to train the model, while temperature values of the other battery data set are used to test model. In Table 1, the data sets used for training and test based on different experiments are given. The process is executed using MATLAB. The training and test processes are detailed here:

4.2.1. Training

- The normalized temperature and capacity values of a battery data set are given as input and target values respectively, for training using NSGA-II to develop optimal parameters (weights, bias, and temperature thresholds).
- Using the optimized temperature thresholds and capacity at each time point, the state machine either switches from one state to another or remains in the same state.
- Based on the selected state, the estimated capacity at that time point is calculated using the NARX model with the optimized weight and bias values.
- By calculating the deviation between the estimated and actual capacity, the objective function is evaluated.

4.2.2. Test

Based on the optimized parameters developed from the training process, the model is tested using the test data set to develop capacity estimations. The actual and estimated capacities are compared for evaluations using RMSE and MSE.

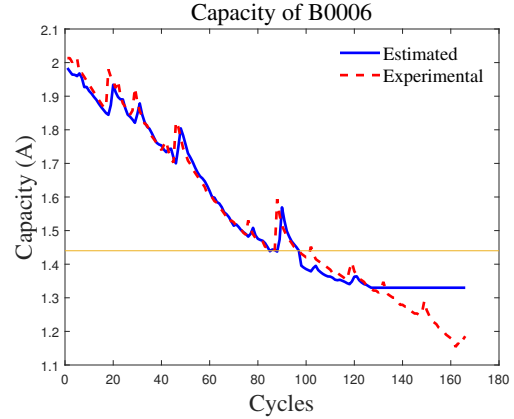


Figure 2. Actual and estimated discharge capacity of B0006.

5. RESULTS

In this section, the estimated capacities based on the different experiments are presented. In addition, the RMSE and MSE values are given. For further insights, the temperature threshold values obtained for each experiment as well as the estimated and actual capacity when the battery reaches EoL (changes to state 2) are given.

5.1. Experiment I results

In Figure 2, the estimated capacity (blue line) and actual capacity (red dotted line) of test data B0006 are shown. The yellow line indicates the EoL capacity (1.44 A). Despite some off trends at the end, the estimated capacity fade curve shows a close proximity to the actual capacity fade. Low RMSE and MSE values of 0.0424 and 0.0043 are achieved based on the proposed approach, showing the model performs well. The state progression is shown in Figure 3. The tr_1 and tr_2 defined by the optimizer are -0.4408 and -1.3387, respectively. Here, it can be observed that the estimation begins with state 1, changes to state 2 (EoL) at cycle 100 (estimated capacity: 1.4335 A) and changes to state 3 at the end. The actual EoL cycle is also 100 (actual capacity: 1.4312 A). The estimated state remains in state 1 until cycle 100 as the threshold conditions for a transition are not met (based on the temperature and capacity at the each specific time point). Once the conditions are met, a change to state 2 can be observed. The estimated state progression is same as the actual state progression of the battery, proving the accuracy of the model.

5.2. Experiment II results

In Figure 4, the estimated capacity of RW9 is close to the actual capacity. The model has a good performance with low RMSE and MSE values (0.0361 and 0.0013). The actual and estimated state profiles are close to each other (Figure 5). The tr_1 and tr_2 defined here are -0.4515 and -1.2338 respectively. The actual EoL is reached at cycle 15 (actual capacity:

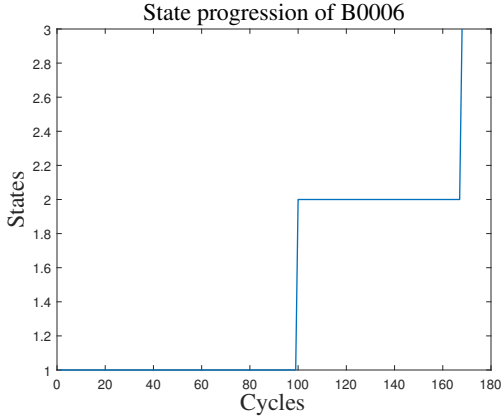


Figure 3. State progression of B0006.

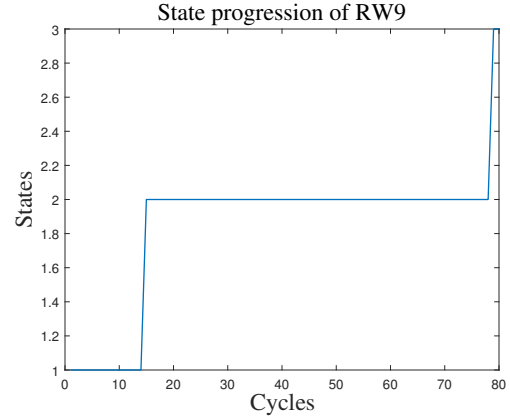


Figure 5. State progression of RW9.

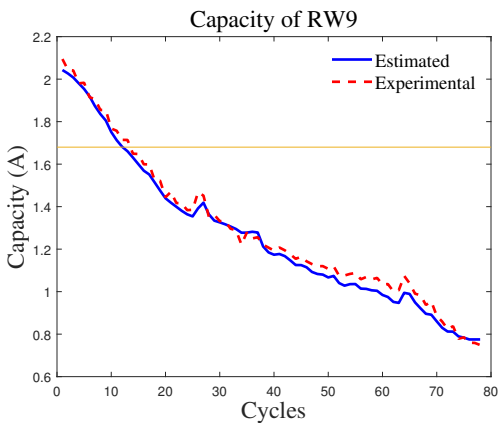


Figure 4. Actual and estimated discharge capacity of RW9.

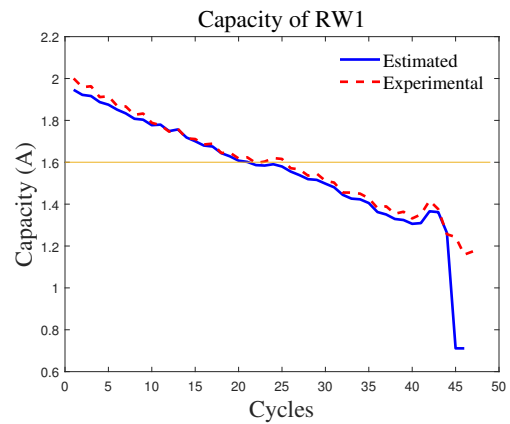


Figure 6. Actual and estimated discharge capacity of RW1.

1.6491 A). The estimated state also switches to state 2 (EoL reached) at cycle 15 (estimated capacity: 1.6402 A). Hence, the model correctly predicts the EoL cycle. The performance of the model also shows that this method is applicable for data with dynamic profiles.

5.3. Experiment III results

The RMSE and MSE values based on RW1 is 0.0337 and 0.0011. The low error rates show that the actual capacity values are close to the estimated values. A deviation is observed in the estimated capacity towards the end, nevertheless the estimation is mostly accurate through the capacity fade (Figure 6). The state progression also shows that the model estimates state one in the beginning and switches to state 2 at cycle 25 (estimated capacity: 1.5732 A), close to the actual EoL cycle (actual capacity: 1.5964 A), which is cycle 23 (Figure 7). The model switches to the final state towards the end of the discharge capacity. The tr_1 and tr_2 developed here are 0.4103 and -1.882, respectively. The model also performs well when applied to this dynamical data.

The results based on the different test data are summarized in

Table 2, which shows the RMSE, MSE, actual, and estimated cycle of EoL state. Based on the generated results, it can be concluded that the proposed model can track the capacity fade effectively. In addition, the model is able to estimate the state progression closely.

Comparisons between the proposed approach and a standard ANN are performed as well to validate the model's performance (Table 3) using the same input variables. The ANN consists a hidden layer of ten neurons. While the standard ANN generates low RMSE and MSE values, the proposed approach achieves a lower RMSE and MSE than the standard ANN for all data sets showing the model's effectiveness. A possible reason for this is due to the advantage of the NARX to handle time series data well.

6. CONCLUSION

In this research, a NARX-based state machine model is developed for the estimation of the capacity fade to evaluate the battery's health. The model does not require electrochemical knowledge, hence eliminating the need for complex formulations. Three damage states and transition conditions be-

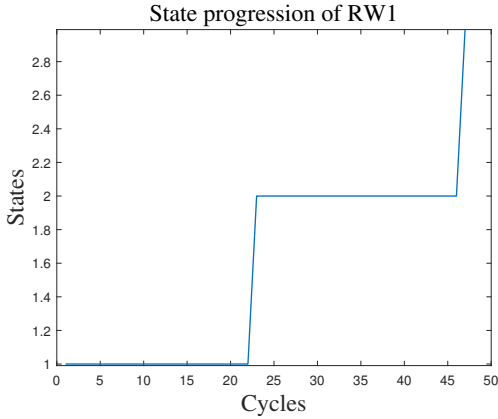


Figure 7. State progression of RW1.

Table 2. Performance of the the model based on different data sets.

Test data	RMSE	MSE	Actual EoL cycle	Estimated EoL cycles
B0006	0.0424	0.0043	100	100
RW9	0.0361	0.0013	15	15
RW1	0.0337	0.0011	25	23

tween the states are defined based on the thresholds of the normalized temperature and capacity (parameters). The state machine switches from state 1 to 2 (indicating EoL), if the threshold conditions are met. Similarly, the model switches from state 2 to 3 based on specific threshold conditions. The discharge capacity of each damage state is calculated using different NARX models with optimized parameters (weight and bias). Optimization of the parameters are performed using NSGA-II. Based on the results, the model is able to estimate the capacity fade accurately for three different experiments with low RMSE (ranging from 0.00337 to 0.0424) and MSE (ranging from 0.0011 to 0.0043) values. The state progression also show close proximity to the actual progression. Comparisons to a standard ANN, show that the proposed approach outperforms the ANN in terms of the RMSE and MSE. In summary, the model is able to perform well for both dynamical and non-dynamical data. In future, the model can be modified by including other variables (such as current) and changing the transition conditions. In addition, more states can be added by expanding the switching behavior between states, as the current model's transitions are limited. For an

Table 3. Performance comparisons between ANN and proposed approach.

Test data	RMSE		MSE	
	Proposed approach	ANN	Proposed approach	ANN
B0006	0.0424	0.1021	0.0043	0.0104
RW9	0.0361	0.1807	0.0013	0.0326
RW1	0.0337	0.2421	0.0011	0.0586

example, including transition from state 1 to 3 and state 2 to 1.

ACKNOWLEDGMENT

This research is partly supported by the German Academic Exchange Service (DAAD) scholarship received by first author for her Ph.D. study at the Chair of Dynamics and Control, University of Duisburg-Essen, Germany.

REFERENCES

- Ashwin, T., Chung, Y. M., & Wang, J. (2016). Capacity fade modelling of lithium-ion battery under cyclic loading conditions. *Journal of Power Sources*, 328, 586-598.
- Beganovic, N., & Söffker, D. (2017). Remaining lifetime modeling using state-of-health estimation. *Mechanical Systems and Signal Processing*, 92, 107-123.
- Bole, B., Kulkarni, C., & Daigle, M. (2014). *Adaptation of an electrochemistry-based li-ion battery model to account for deterioration observed under randomized use*, annual conference of the prognostics and health management society. NASA Prognostics Data Repository, NASA Ames Research Center, Moffett Field, CA.
- Catelani, M., Ciani, L., Fantacci, R., Patrizi, G., & Picano, B. (2021). Remaining useful life estimation for prognostics of lithium-ion batteries based on recurrent neural network. *IEEE Transactions on Instrumentation and Measurement*, 70, 1-11.
- Chan, R. W., Yuen, J. K., Lee, E. W., & Arashpour, M. (2015). Application of nonlinear-autoregressive-exogenous model to predict the hysteretic behaviour of passive control systems. *Engineering Structures*, 85, 1-10.
- Christensen, J., & Newman, J. (2003). Effect of anode film resistance on the charge/discharge capacity of a lithium-ion battery. *Journal of The Electrochemical Society*, 150(11), A1416.
- Daigle, M., & Kulkarni, C. S. (2013). Electrochemistry-based battery modeling for prognostics. In *Annual Conference of the PHM Society*.
- David, R., Rothe, S., & Söffker, D. (2021). Lane changing behavior recognition based on artificial neural network-based state machine approach. In *2021 IEEE International Intelligent Transportation Systems conference (ITSC)* (p. 3444-3449).
- Deb, K., Pratap, A., Agarwal, S., & Meyarivan, T. (2002). A fast and elitist multiobjective genetic algorithm: Nsgaii. *IEEE Transactions on Evolutionary Computation*, 6(2), 182-197.
- Downey, A., Lui, Y.-H., Hu, C., Laflamme, S., & Hu, S. (2019). Physics-based prognostics of lithium-ion battery using non-linear least squares with dynamic bounds. *Reliability Engineering System Safety*, 182,

- 1-12.
- Gill, A. (1962). *Introduction to the theory of finite-state machines*. McGraw-Hill.
- Horne, B., & Giles, C. (1994). An experimental comparison of recurrent neural networks. *Advances in neural information processing systems*, 7, 697–704.
- Hu, X., Zou, C., Zhang, C., & Li, Y. (2017). Technological developments in batteries: A survey of principal roles, types, and management needs. *IEEE Power and Energy Magazine*, 15(5), 20-31.
- Keil, P., & Jossen, A. (2017). Impact of dynamic driving loads and regenerative braking on the aging of lithium-ion batteries in electric vehicles. *Journal of The Electrochemical Society*, 164, A3081-A3092.
- Kögler, F., & Söffker, D. (2020). State-based open-loop control of plant growth by means of water stress training. *Agricultural Water Management*, 230, 105963.
- Liu, Z., Sun, G., Bu, S., Han, J., Tang, X., & Pecht, M. (2017). Particle learning framework for estimating the remaining useful life of lithium-ion batteries. *IEEE Transactions on Instrumentation and Measurement*, 66(2), 280-293.
- Lopes, S. F., Silva, S., & Monteiro, J. L. (2012). An easy-to-use and flexible object-oriented framework for extended finite state machines. In *IEEE 10th International Conference on Industrial Informatics* (p. 35-40).
- Álvarez Antón, J. C., García Nieto, P. J., García Gonzalo, E., Viera Pérez, J. C., González Vega, M., & Blanco Viejo, C. (2016). A new predictive model for the state-of-charge of a high-power lithium-ion cell based on a pso-optimized multivariate adaptive regression spline approach. *IEEE Transactions on Vehicular Technology*, 65(6), 4197-4208.
- Micheli, G. D., Brayton, R. K., & Sangiovanni-Vincentelli, A. L. (1985). Optimal state assignment for finite state machines. *IEEE Transactions on Computer-Aided Design of Integrated Circuits and Systems*, 4, 269-285.
- Patil, M. A., Tagade, P., Hariharan, K. S., Kolake, S. M., Song, T., Yeo, T., & Doo, S. (2015). A novel multistage support vector machine based approach for li ion battery remaining useful life estimation. *Applied Energy*, 159, 285-297.
- Plett, G. L. (2004). Extended kalman filtering for battery management systems of lipb-based hev battery packs: Part 2. modeling and identification. *Journal of Power Sources*, 134(2), 262-276.
- Saha, B., & Goebel, K. (2007). *Battery data set*. NASA Prognostics Data Repository, NASA Ames Research Center, Moffett Field, CA.
- Saha, B., & Goebel, K. (2009). Modeling li-ion battery capacity depletion in a particle filtering framework. In *Annual Conference of the PHM Society*.
- Siegelmann, H., Horne, B., & Giles, C. (1997). Computational capabilities of recurrent narx neural networks. *IEEE Transactions on Systems, Man, and Cybernetics, Part B (Cybernetics)*, 27(2), 208-215.
- Thangaraj, R., Pant, M., Abraham, A., & Snasel, V. (2012). Modified particle swarm optimization with time varying velocity vector. *International Journal of Innovative Computing, Information and Control*, 8(1), 201–218.
- Venturini, M. (2005). Simulation of Compressor Transient Behavior Through Recurrent Neural Network Models. *Journal of Turbomachinery*, 128(3), 444-454.
- Waldmann, T., Wilka, M., Kasper, M., Fleischhammer, M., & Wohlfahrt-Mehrens, M. (2014). Temperature dependent ageing mechanisms in lithium-ion batteries – a post-mortem study. *Journal of Power Sources*, 262, 129-135.
- Wang, J., Liu, P., Hicks-Garner, J., Sherman, E., Soukiazian, S., Verbrugge, M., ... Finamore, P. (2011). Cycle-life model for graphite-lifepo 4 cells. *Lancet*, 196, 3942-3948.
- Wilson, P., & Mantooth, H. A. (2013). *Chapter 6 - block diagram modeling and system analysis* (P. Wilson & H. A. Mantooth, Eds.). Oxford: Newnes. doi: <https://doi.org/10.1016/B978-0-12-385085-0.00006-3>
- Wu, J., Kong, L., Cheng, Z., Yang, Y., & Zuo, H. (2022). Rul prediction for lithium batteries using a novel ensemble learning method. *Energy Reports*, 8, 313-326. (2022 International Conference on the Energy Internet and Energy Interactive Technology)
- Wu, Y., Li, W., Wang, Y., & Zhang, K. (2019). Remaining useful life prediction of lithium-ion batteries using neural network and bat-based particle filter. *IEEE Access*, 7, 54843-54854.
- Xiao, Y. (2015). Model-based virtual thermal sensors for lithium-ion battery in ev applications. *IEEE Transactions on Industrial Electronics*, 62, 3112-3122.
- Xu, X., & Chen, N. (2017). A state-space-based prognostics model for lithium-ion battery degradation. *Reliability Engineering System Safety*, 159, 47-57.
- Zhang, H., Wu, D., Wang, Z., & Chen, Y. (2021). An ensemble method for the heterogeneous neural network to predict the remaining useful life of lithium-ion battery. In *2021 IEEE International Conference on Systems, Man, and Cybernetics (SMC)* (pp. 2433–2438).
- Zhao, S., Zhang, C., & Wang, Y. (2022). Lithium-ion battery capacity and remaining useful life prediction using board learning system and long short-term memory neural network. *Journal of Energy Storage*, 52, 104901.
- Zheng, L., Zhang, L., Zhu, J., Wang, G., & Jiang, J. (2016). Co-estimation of state-of-charge, capacity and resistance for lithium-ion batteries based on a high-fidelity electrochemical model. *Applied Energy*, 180, 424-434.

BIOGRAPHIES



Ruth David is currently pursuing her Ph.D. degree with the Chair of Dynamics and Control, University of Duisburg-Essen, Germany. Her current research interests include recognition and prediction of driving behaviors based on applications of machine learning methods. She currently focuses on developing a state machine-based model as a new machine learning approach for the prediction and recognition of behaviors.



Dirk Söffker received his Dr.-Ing. degree in safety engineering and the Habilitation degree in automatic control/safety engineering from University of Wuppertal, Germany, in 1995 and 2001, respectively. Since 2001, he leads the Chair of Dynamics and Control, University of Duisburg-Essen, Germany. His current research interests include diagnostics and prognostics, modern methods of control theory, human interaction with safe human interaction with technical systems, safety and reliability control engineering of technical systems, and cognitive technical systems. Since 2023, he serves as the Head of the Mechanical and Process Engineering Department and as Vice Dean of the Faculty of Engineering responsible for the Mechanical Engineering department.